Phasing methods of tiled-aperture coherent beam combining for high peak power lasers

Chun Peng[1,2], *Xiaoyan* Liang[1,3,4,*], *Renqi* Liu[1,2], *Wenqi* Li[1,2,4], *Ruxin* Li[1,3,4]

[1]State Key Laboratory of High Field Laser Physics, Shanghai Institute of Optics and Fine Mechanics, Chinese Academy of Sciences,Shanghai 201800, China
[2]University of Chinese Academy of Sciences, Beijing 100049, China
[3]IFSA Collaborative Innovation Center, Shanghai Jiao Tong University, Shanghai 200240, China
[4]School of Physical Science and Technology, ShanghaiTech University, Shanghai 200031, China

Abstract. We demonstrate two type phasing methods for tiled-aperture coherent beam combining for high-power lasers based on the near and far field measurement techniques respectively, a comparison is made.

1 Introduction

Coherent beam combining (CBC) has been considered as a promising way to scale the output capacity of a single laser system, which breaking through the limitations caused by thermal behaviour of gain medium, optical damage threshold of materials and optical coatings, or detrimental nonlinear effects [1]. Recently, CBC of tiled aperture configuration based on active phasing method has been extended to the generation of high peak power laser pulses by the pursuit of extreme intense conditions owing to its ability to achieve N^2 (N is the number of the combined beams) times peak intensity in the focal plane [2,3]. For this purpose, the primary but the most challenging issue lies in keeping the zeroth-order phases actively stabilized. In this contribution, we present different phasing methods based on the near and far field measurement techniques respectively to find an appropriate phasing solution for tiled-aperture CBC in the high peak power regime.

2 Experiments and results

The phasing methods were demonstrated on a Ti:Sapphire laser delivering femtosecond pulses at a central wavelength of 800 nm with a FWHM bandwidth of 15 nm and a repetition rate of 1 kHz. The duration of the laser pulses was 50 fs, the diameter was 5 mm, and the energy of a single pulse was approximately 0.5 mJ. Fig. 1(a) and Fig. 2(a) show the experimental setups for two-beam CBC based on the near-field measurement technique and the far-field measurement technique, respectively. In these two structures, the spatial collimation was realized by mirror mounts and a tip-tilt mirror owing to the near- and far-field distributions. The time domain synchronization was controlled by a piezo-electric transducer (PZT) platform in DL1 by adjusting the optical length of the beam. The

* Corresponding author: liangxy@siom.ac.cn

synchronization error was diagnosed by the measurement units and delivered to the processing module, wherein the program calculated the error signal and fed it back to the PZT in real time. Camera 2 is a high-speed monochrome camera with a maximum frame rate of 543 fps at the full resolution of 1696 × 1704 pixels, which can be further improved to more than 4K fps by reducing the frame resolution. The combined beam pattern was recorded by camera 1.

In Fig. 1(a), a hybrid phasing method based on the near-field interference fringe (NIFF) technique and single crystal balanced optical cross-correlation (BOC) is used. We realized an adjustable beam combining bandwidth of approximately 100 Hz (limited by the speed of the PZT) and root-mean-square deviation of approximately$\lambda/51$ (shown in Fig. 1(b)) for two beam channels with a combining efficiency of 93%.

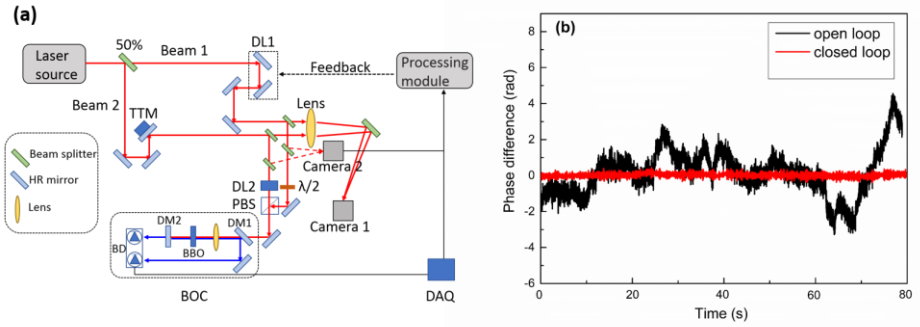

Fig. 1. (a)Experiment setup. BD, balanced photodetector; BOC, balanced optical cross-correlator; DL1/DL2, delay line; DM1, dichroic mirror, AR at 800 nm, HR at 400 nm; DM2, dichroic mirror, AR at 400 nm, HR at 800 nm; PBS, polarization beam splitter; TTM, tip-tilt mirror; BBO, beta barium borate crystal; DAQ, data acquisition card. (b) Phase errors recorded in an open loop and closed loop.

In Fig. 2(a), the phasing technique is based on the far-field interference fringe measurement. The phase error is diagnosed directly from the far-field of the tiled-aperture CBC where the coherent combination happens. The bandwidth is approximately 100 Hz which is limited by the speed of PZT. The phase error is controlled with an RMS deviation of 0.157 rad (approximately 1/40 λ), shown in Fig. 2(b), the coherently combined beam pattern corresponding to a coherent efficiency of 92%.

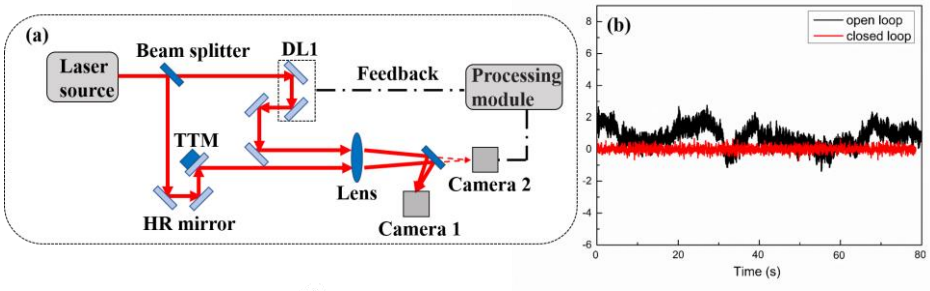

Fig. 2. (a) Experiment setup. DL1 is delay line, HR mirror is high reflected mirror, and TTM is tip-tilt mirror. (b) Phase errors recorded in the open loop and closed loop.

Comparing these two structures, we can see that the phase error of tiled-aperture CBC can be diagnosed from whether the near-field or the far-field. Phasing method based on the near-field measurement is more convenient to adjust and possesses better accuracy. The

latter one based on the far-field measurement has simpler optical structure but with higher algorithm requirement, the measurement accuracy is also limited by the resolution of Camera 2. But detecting the phase error from the far-field offers a direct observation of the coherent combination effect and realize a full-path error measurement for the reason that the ultra-intense field is created in the focal plane. Moreover, the phase error of tiled-aperture can be detected by translated into electrical signal (the BOC [4] and Hansch-Couillasud detectors [2]) or image signal (interference fringe detector [5]). Combining different type approaches can raise the anti-disturbing capacity of the system.

3 Conclusion

To summarized, we present different implementations of phasing method for tiled-aperture CBC based on the near-field and far-field measurement techniques. In the proof-of-principle experiment, all these meet the phase control requirement of femtosecond pulses CBC. The merit and demerit is compared.

References

1. T. Y. Fan, IEEE J. Sel. Top. Quantum Electron. **11**, 567, Jun. (2005).
2. S. Bagayev, V. Leshchenko, V. Trunov, E. Pestryakov, and S. Frolov, Opt. Lett. **39**, 6, 1517 (2014).
3. J.-P. Chambaret, O. Chekhlov, G. Chériaux, J. Collier, R. Dabu, P.Dombi, A. M. Dunne, K. Ertel, P. Georges, J. Hebling, J. Hein,C.Hernandez-Gomez, C. Hooker, S. Karsch, G. Korn, F. Krausz, C.Le Blanc, Z. Major, F. Mathieu, T. Metzger, G. Mourou, P. Nickles,K. Osvay, B. Rus, W. Sandner, G. Szabó, D. Ursescu, and K.Varjú, Proc. SPIE **7721**, 77211D (2010).
4. S.-W. Huang, G. Cirmi, J. Moses, K.-H. Hong, S. Bhardwaj, J. R. Birge, L.-J. Chen, E. Li, B. J. Eggleton, G. Cerullo, and F. X. Kärtner, Nat. Photonics **5**, 475 (2011).
5. C. Peng, X. Liang, R. Liu, W. Li, and R. Li, Opt. Lett. **42**, 3960 (2017).